Theoretical Study of the Structural and Fluxional Behavior of Copper(I)-Octahydrotriborate Complex

C. Serrar, A. Es-sofi, A. Boutalib,* A. Ouassas, and A. Jarid

Département de Chimie, Université Cadi Ayyad, Faculté des Sciences Semlalia, B.P. 2390, Marrakech, Morocco

I. Nebot-Gil and F. Tomás

Institut de Ciència Molecular (Departament de Química-Física), Universitat de València, Dr. Moliner, 50 E−46100, Burjassot, València, Spain

Received: May 7, 2001; In Final Form: July 5, 2001

The geometrical structures of $[B_3H_8]^-$ and $[ClCuB_3H_8]^-$ compounds have been investigated by means of ab initio calculations, using the MP2 level of theory, and density functional theory (DFT) method. The $[ClCuB_3H_8]^-$ (**3a**) complex structure, in which two boron atoms were bound to the copper atom via two B−H−Cu bridge hydrogen bonds (one bridge bond for each boron), was the most stable. Its MP2 and DFT calculated geometry is comparable to that of B_4H_{10}. In addition, the DFT calculated vibrational frequencies are in good agreement with experimental values. On the other hand, the most favorable interconversion of **3a** structure was found to proceed with a low activation barrier (6.5 kcal mol^{-1}). This is consistent with the NMR spectra and confirms the rapid fluxional behavior for this complex. Moreover, the isomerization leading to **3a**, from the less stable structure **3c**, also proceeds with a low energy barrier (5.2 kcal mol^{-1}), whereas the activation barrier of reverse rearrangement is negligible. The calculated energy barriers of the rearrangement between the less stable structures **3b** and **3c** are also very small (1.2 kcal mol^{-1}).

Introduction

In general, the octahydrotriborate (1−) anion, $[B_3H_8]^-$ plays an important role, as ligand, in the synthesis of metalatetraboranes. In this case, a number of metal octahydrotriborate complexes have been reported.[1−16] Several of these species are known to be fluxional. The mobility of the hydrogens, as observed by NMR spectra, further complicates the structural analysis for these compounds. In our recent paper, we have described the preparation of the new copper (I) complex $[R_4N][ClCuB_3H_8]$ (R = Et, n-Pr, n-Bu).[17] Its ^{11}B and ^1H NMR spectra, in solution, show that all protons and borons remain equivalent on the NMR time scale down to −50 °C. This indicates the rapid fluxional behavior of this complex in solution. This character is similar to that observed in free $[B_3H_8]^-$ anion[18] and in other octahydrotriborate complexes[7−10] On the other hand, the infrared spectrum of [n-Bu][$ClCuB_3H_8$] exhibits the presence of the bridging (B−H−B) and terminal (B−H) hydrogens.

To explain these experimental observations and to propose an accurate structure for the $[ClCuB_3H_8]^-$ anion, we have examined, several structures for this complex using ab initio and DFT calculations. Its transition states for the possible rearrangements are located. The optimized geometry parameters of different stationary points are reported. To interpret the fluxional behavior of the $[ClCuB_3H_8]^-$ complex, we propose a possible mechanism for its isomerization.

Computational Methods

All calculations were performed using the GAUSSIAN 94 program package[19] on the workstations (IBM RS/6000) of the University of València.

The basis sets used were 6-31G** for H and B atoms, and 3-21G* for Cu and Cl atoms. All geometries were optimized at MP2 and DFT (B3LYP)[20−22] levels. Each stationary point found has been classified as either a minimum or transition state, if its Hessian matrix of energy second derivatives shows zero or one (and only one) negative eigenvalues, respectively. The intrinsic reaction coordinate (IRC)[23,24] algorithm was used to verify the structures connected by the transition states. DFT vibrational frequencies have been calculated and compared to those found experimentally. The electronic structures were analyzed by using the natural bond orbital NBO[25] partitioning scheme.

Results and Discussion

Optimized geometries of different stationary points considered in this study are shown in Figures 1 and 2. Their calculated relative energies are listed in Table 1. These values are relative to the most stable structure (**3a**). Selected optimized bond lengths for $[B_3H_8]^-$ and $[B_4H_{10}]$ structures, $[ClCuB_3H_8]^-$ structures (**3a**−**3c**), and all located transition structures (**TS_1**−**TS_5**) are reported in Tables 2, 3, and 4, respectively.

For the first time, we have optimized the geometries for the double- and single-bridge hydrogen **1a** and **1b** structures of $[B_3H_8]^-$ anion at both MP2 and DFT levels (Figure 1). We have found the X-ray crystal structure of the first structure.[26−28] All of our calculations show that the **1a** structure is a minimum and the **1b** a transition state in the total-potential-energy surface. The **1b** structure is higher in energy than **1a** by only 2.3 and 1.4 kcal mol^{-1} at MP2 and DFT levels, respectively. This result, which is in good agreement with other previous calculations,[29−31] confirms the marked fluxional behavior of this anion.

In the case of the $[ClCuB_3H_8]^-$ complex, three structures **3a**, **3b,** and **3c** (Figure 2) have been considered and optimized

* Corresponding author. E-mail: boutalib@ucam.ac.ma.

10.1021/jp0117314 CCC: $20.00
Published on Web 09/29/2001

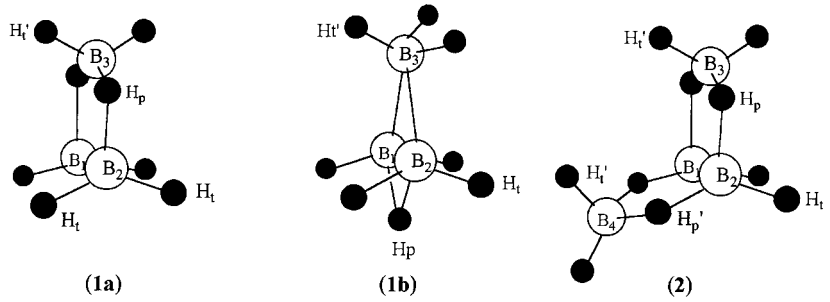

Figure 1. Optimized structures for $[B_3H_8]^-$ (**1a** and **1b**) and B_4H_{10} (**2**).

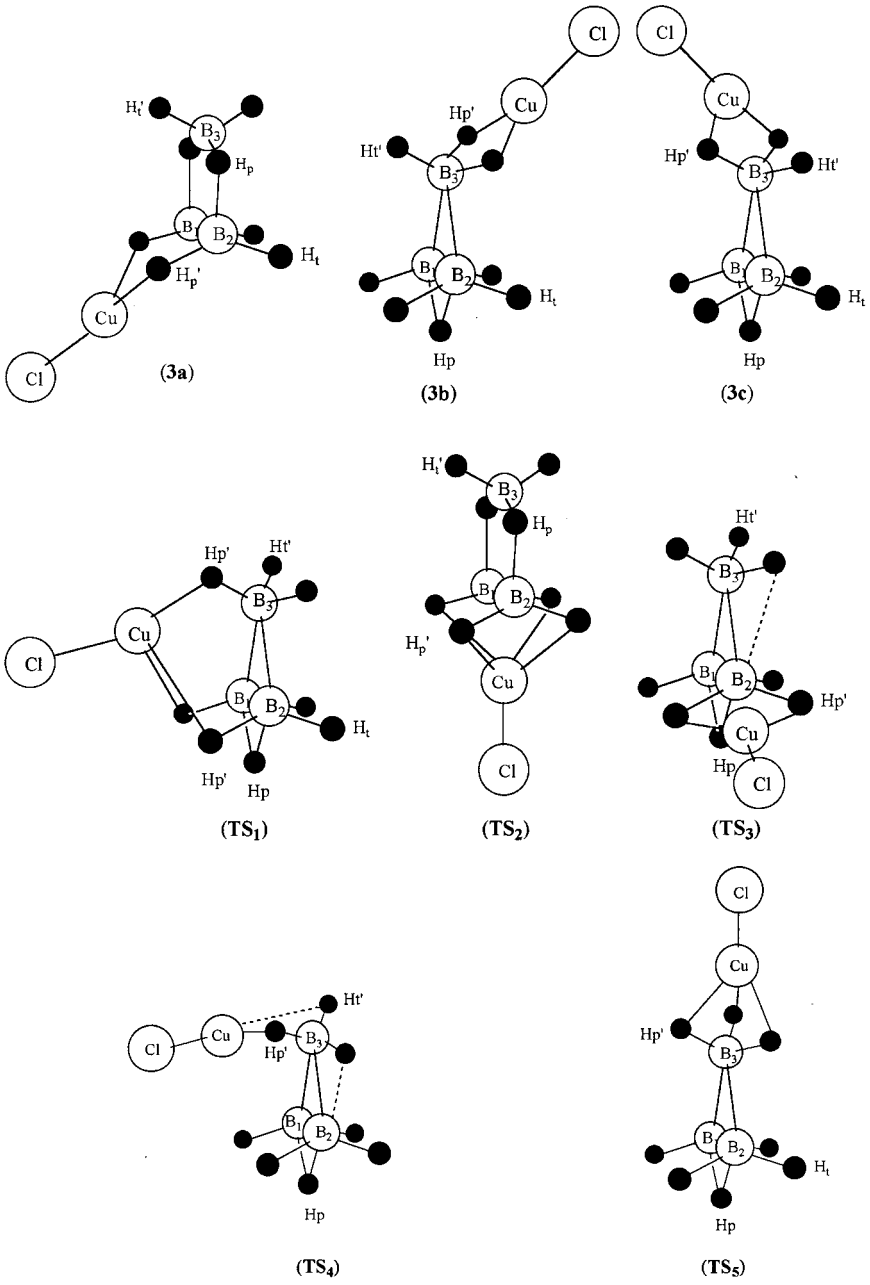

Figure 2. Optimized structures for $[ClCuB_3H_8]^-$ (**3a**-**3c**, **TS1**-**TS5**).

at the same levels of theory. These structures are the true minima in the total-potential-energy surface. The **3a** conformation differs essentially from **3b** and **3c** by the structure of the $[B_3H_8]^-$ ligand and by the number of boron atoms coordinated to the copper atom. In the **3a** structure, the $[B_3H_8]^-$ ligand has a double-bridge structure and is bound to the metal by two different boron atoms, through two B−H−Cu bridging hydrogen bonds. In the **3b** and **3c** structures the $[B_3H_8]^-$ ligand has one B−H−B bridged hydrogen and is coordinated to the Cu center by only one boron atom. The **3b** structure differs essentially from **3c** by the position of the CuCl bond. Indeed, in the **3b** structure the CuCl bond is in a perpendicular plane to that formed by $B_1B_2B_3$, while in

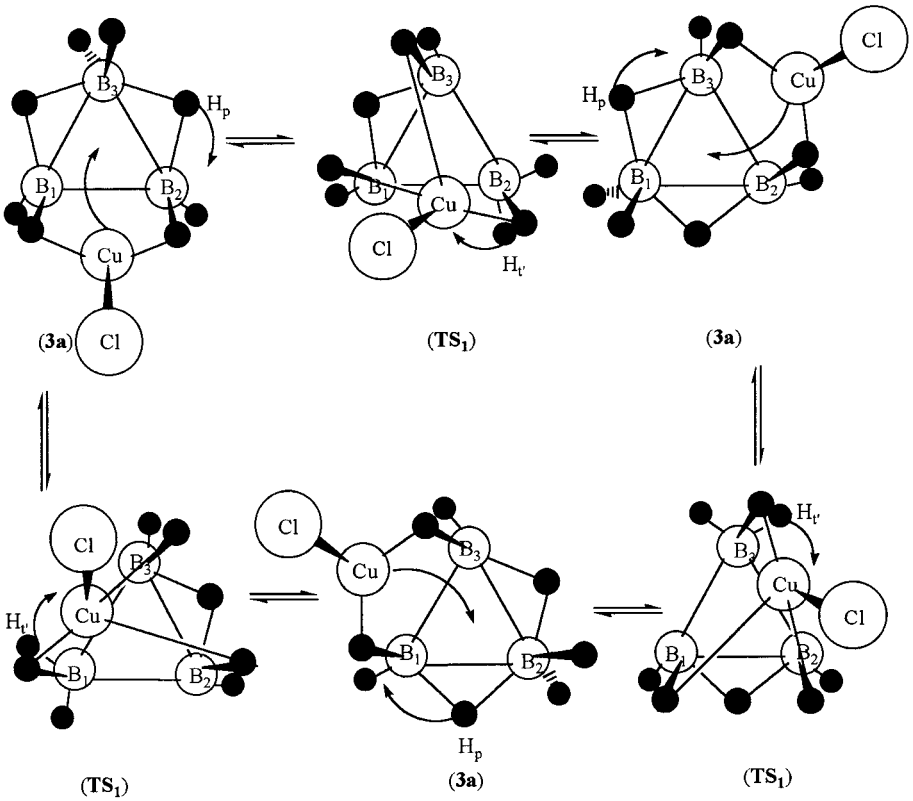

Figure 3. Interconversion of 3a structure through $\mathbf{TS_1}$ transition state.

TABLE 1: MP2 and DFT Absolute Energies (au) and Relative Energies (kcal mol^{-1}) of Different Structures of $[ClCuB_3H_8]^-$

Structure	MP2	DFT
E**(3a)**	−2167.88425	−2170.16752
3b	4.56	2.97
3c	5.13	2.67
$\mathbf{TS_1}$	6.33	4.00
$\mathbf{TS_2}$	10.15	7.27
$\mathbf{TS_3}$	13.93	10.50
$\mathbf{TS_4}$	5.18	2.85
$\mathbf{TS_5}$	5.74	3.30

the **3c** structure, the CuCl bond is in a nonperpendicular one. On the other hand, the calculated relative energies, reported in Table 1, indicate that the **3a** structure is more stable than both the **3b** and **3c** structures at all levels. These two latter structures are energetically close. The **3b** structure was found lower in energy than **3c** by about 0.5 kcal mol^{-1} at MP2 level. Nevertheless, the DFT calculations reverse this order, showing that the **3c** structure is slightly more stable than **3b** by about 0.3 kcal mol^{-1}. In the **3a** structure, the MP2 and DFT calculated bond length B_1B_2 (1.798 and 1.809 Å, respectively) is slightly shorter than the bridging bond length B_1B_3 (1.802 and 1.816 Å, respectively). In contrast, the scenario is reversed in the **1a** structure of the free $[B_3H_8]^-$ anion (B_1B_2 is 1.824 and 1.846 Å, and B_1B_3 is 1.783 and 1.792 Å at the MP2 and DFT levels, respectively). This trend in boron−boron bond lengths, obtained on going from the free $[B_3H_8]^-$ to $[ClCuB_3H_8]^-$, is analogous to that found in B_4H_{10} (**2**) (Table 2). This is in agreement with the fact that the **3a** structure is derived from B_4H_{10},[32] in which the $[BH_2]^+$ group is replaced by the CuCl fragment. We have also noted that, in the **3a** structure, the Cu atom is out of the B_1, B_2 and the bridging hydrogens H_p' plane. The calculated dihedral angle between the Cu atom and the $B_1B_2H_p$' plane is around 41° at the MP2 and DFT levels. This atomic disposition, which stabilizes the **3a** conformation, is probably a result of the slight interaction between the Cu metal and two boron atoms of the unbridged bond. Then, to verify this hypothesis, we have calculated the NBO charges for the **1a** structure of the free $[B_3H_8]^-$ and the **3a** structure of the $[ClCuB_3H_8]^-$ complex, using the same levels of calculation. The results indicate a slight variation of B_1 and B_2 atom charges on going from the free $[B_3H_8]^-$ (**1a**) to $[ClCuB_3H_8]^-$ (**3a**) (from −0.39 to −0.48 e and from −0.45 to −0.54 e at MP2 and DFT levels, respectively). Otherwise, the stability of **3a** may be explained also by the fact that in the free $[B_3H_8]^-$ anion (**1a**), the B_1 and B_2 atoms are richer in electrons than the B_3 atom (−0.15 and −0.26 e at MP2 and DFT levels, respectively). Therefore, the attack of the Cu center on the unbridged bond, B_1B_2, is most favorable.

TABLE 2: Selected Interatomic Distances (Å) for $[B_3H_8]^-$ and B_4H_{10} Structures

	$[B_3H_8]^-$					B_4H_{10}		
	1		**1b**			**2**		
	MP2	DFT	MP2	DFT	expt[a]	MP2	DFT	expt[b]
B_1B_2	1.824	1.846	1.716	1.728	1.80	1.720	1.722	1.75
B_1B_3	1.783	1.792	1.855	1.873	1.77	1.842	1.862	1.845
B_1H_p	1.257	1.262	1.328	1.337	1.20	1.246	1.257	1.21
B_3H_p	1.465	1.494			1.50	1.408	1.413	1.37
B_1H_t	1.203	1.210	1.201	1.208	1.05−1.2	1.178	1.184	1.05−1.17
$B_3H_{t'}$	1.205	1.211	1.213	1.217	1.05−1.2	1.190	1.195	1.05−1.17
$B_1H_{p'}$						1.246	1.257	1.21
$H_{p'}B_4$						1.408	1.413	1.37
B_1B_4						1.842	1.862	1.840

[a] Reference 27. [b] Reference 32.

The DFT unscaled vibrational frequencies of the **3a** structure, in the 2000−2600 cm^{-1} range, are in agreement with those obtained experimentally for $[(n\text{-}Bu)_4N][ClCuB_3H_8]$ salt. These calculated frequencies are also in good agreement with the observed ones of the $(PPh_3)_2CuB_3H_8$ complex.[7] Our theoretical study also predicts a high absolute value of the $[ClCuB_3H_8]^-$ (**3a**) complexation energy (−70.3 and −69.82 kcal mol^{-1} at the MP2 and DFT levels, respectively). These values indicate

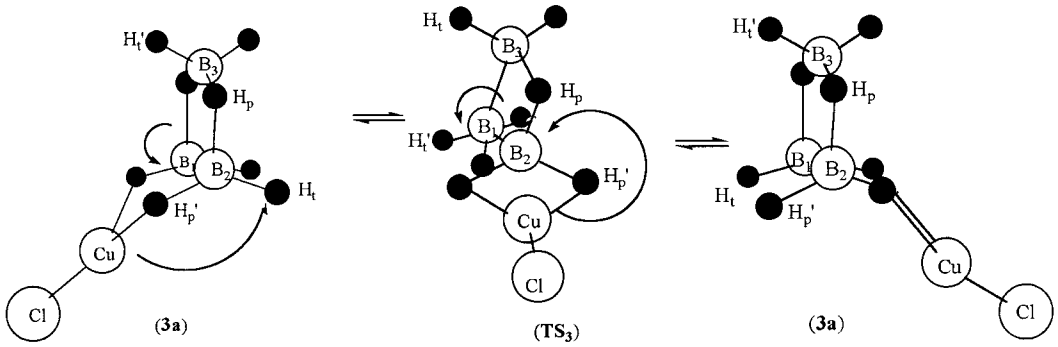

Figure 4. Interconversion of 3a structures through $\mathbf{TS_3}$ transition state.

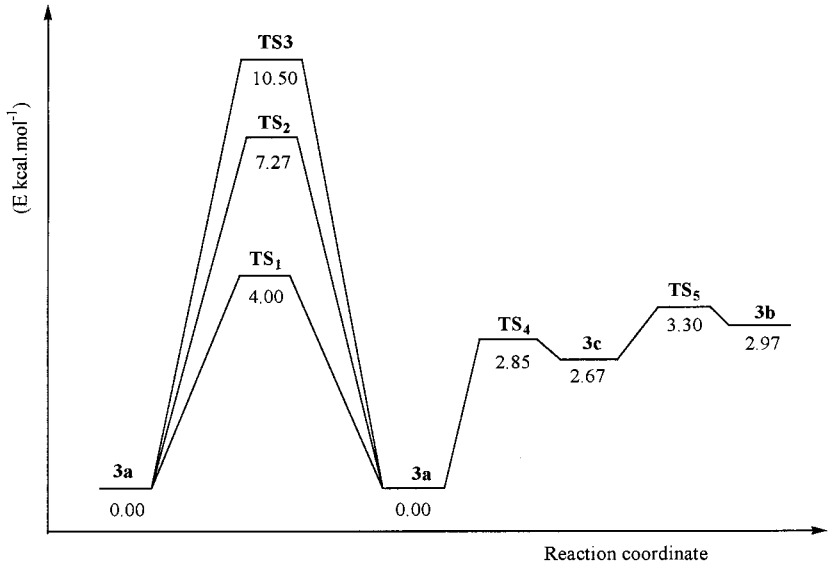

Figure 5. Energy profile building of $[ClCuB_3H_8]^-$ (**3a**) isomerization.

TABLE 3: Selected Interatomic Distances (Å) for $[ClCuB_3H_8]^-$ Structures (3a−3c)

	$[ClCuB_3H_8]^-$					
	3a		**3b**		**3c**	
	MP2	DFT	MP2	DFT	MP2	DFT
B_1B_2	1.798	1.809	1.738	1.749	1.722	1.730
B_1B_3	1.802	1.816	1.846	1.856	1.858	1.869
B_1H_p	1.249	1.257	1.313	1.323	1.308	1.312
B_3H_p	1.436	1.447				
B_1H_t	1.192	1.199	1.195	1.200	1.202	1.209
$B_3H_{t'}$	1.198	1.203	1.196	1.202	1.199	1.206
$B_1H_{p'}$	1.246	1.252				
$B_3H_{p'}$			1.245	1.255	1.227	1.223
					1.254	1.270
$H_{p'}Cu$	1.742	1.764	1.761	1.773	1.964	2.124
					1.669	1.651
B_1Cu	2.199	2.227				
B_3Cu			2.116	2.113	2.102	2.142
CuCl	2.188	2.203	2.158	2.169	2.159	2.177
	2.118[a]	2.109[a]				

[a] Calculated distance of free CuCl.

that the Cu atom is strongly bound to the $[B_3H_8]^-$ ligand. This is confirmed by the calculated Cu−Cl bond length, which increases on going from the free CuCl (2.118 and 2.109 Å at the MP2 and DFT levels, respectively) to the **3a** structure (2.203 and 2.188 Å at the MP2 and DFT levels, respectively). This can be also shown by the Cu−Hp' bond distances (1.742 and 1.764 Å at the MP2 and DFT levels, respectively) which are close to that found in X-ray structure of the $(PPh_3)_2CuB_3H_8$ complex (1.85 Å).[9] However, these results support the proposed **3a** structure for this complex.

To highlight the fluxional behavior of the $[ClCuB_3H_8]^-$ complex and to clarify its rearrangement mechanism, we have carried out a geometrical optimization on the total-potential-energy surface taking into account all the possible rotations of the CuCl fragment vis-à-vis to $[B_3H_8]^-$ one. We have thus localized five transition states $\mathbf{TS_1}$−$\mathbf{TS_5}$ reported in Figure 2. $\mathbf{TS_1}$ is characterized by one bridged hydrogen between two boron atoms (B−H−B) and three bridged bonds B−H−Cu (η^3 coordination mode). The MP2 and DFT distances B_1-H_p' and B_2-H_p' (1.203 and 1.208 Å, respectively) are shorter than B_3-H_p' (1.263 and 1.27 Å, respectively). In addition, the B_1−Cu and B_2−Cu bond lengths (2.67 Å) are greater than the B_3−Cu one (2.27 Å). These values indicate that the B_3 boron is more strongly bound to Cu metal than B_1 and B_2 atoms. However, the $\mathbf{TS_2}$ structure has two bridged hydrogens (B−H−B) and four bridged bonds B−H−Cu (η^4 coordination mode). Thus, the three borons, the two bridged hydrogens, and the Cu and Cl atoms are nearly situated in the same plane. In the $\mathbf{TS_3}$ and $\mathbf{TS_4}$ structures, the $[B_3H_8]^-$ ligand, which is intermediate between the single- and double-bridged structure, has an η^2 coordination mode toward the Cu atom. In addition, the two B_3-H_p' bond lengths of the $\mathbf{TS_3}$ and $\mathbf{TS_4}$ geometries are slightly different. This difference, which becomes significant for the H_p'−Cu bond lengths, is indicative of unsymmetrical binding of copper to the B_3 boron atom (see Table 4). The TS_5 transition state structure has only one bridged hydrogen and three bridged bonds B−H−Cu at the B_3 boron atom. We have remarked that this latter shows a slight tendency to be like the **3c** structure. On the other hand, we have found that $\mathbf{TS_1}$ is a transition state

TABLE 4: Selected Interatomic Distances (Å) for Transition State Structures (TS_1−TS_5)

	Transition State Structures									
	TS_1		**TS_2**		**TS_3**		**TS_4**		**TS_5**	
	MP2	DFT	MP2	DFT	MP2	DFT	MP2	DFT	MP2	DFT
B_1B_2	1.726	1.738	1.798	1.816	1.869	1.887	1.730	1.747	1.746	1.766
B_1B_3	1.856	1.860	1.845	1.862	1.791	1.796	1.852	1.859	1.812	1.836
B_1H_p	1.317	1.327	1.257	1.267	1.323	1.318	1.290	1.289	1.349	1.359
B_3H_p			1.383	1.392	1.337	1.366	1.345	1.371		
B_1H_t	1.174	1.200			1.202	1.206	1.194	1.199	1.195	1.201
							1.206	1.215		
$B_3H_{t'}$	1.201	1.207	1.198	1.203			1.202	1.209	1.206	1.202
$B_1H_{p'}$	1.203	1.208	1.206	1.213						
$B_3H_{p'}$	1.263	1.278			1.219	1.222	1.202	1.209	1.236	1.235
					1.249	1.261	1.257	1.272	1.237	1.270
$H_{p'}Cu$	1.603	1.614	2.355	2.353	1.668	1.661	1.652	1.644	1.773	1.633
	2.325	2.330			1.942	1.993	2.134	2.202	1.776	2.108
B_1Cu	2.669	2.677	2.129	2.123						
B_3Cu	2.262	2.276			2.203	2.128	2.100	2.146	2.030	2.143
CuCl	2.165	2.181	2.186	2.172	2.146	2.155	2.162	2.179	2.159	2.164

between interconverting **3a** structures. In addition, this conversion results from an intramolecular exchange between the bridged and terminal hydrogens, which is accompanied by a change of the $[B_3H_8]^-$ coordination position with the Cu metal (Figure 2). Such an exchange would render the three boron atoms and all protons magnetically equivalent. The calculated activation energy barrier for this process is about 6 and 4 kcal mol^{-1} at MP2 and DFT levels, respectively. These results, which are in good agreement with the NMR spectra, favor this mechanistic model and confirm the fluxional behavior for the $[ClCuB_3H_8]^-$ complex. Moreover, these results indicate also that the internal rearrangement among the **3a** structures through the **TS_2** transition state involves the rotation of the ClCu group around the B_1-B_2 axis without any exchange of hydrogen atoms. The activation energy barrier for this rotation is 10.15 and 7.27 kcal mol^{-1} at the MP2 and DFT levels, respectively. We have also found another way for the internal rearrangement among the **3a** structure through the **TS_3** transition state. This conversion is characterized by the rotation of the $ClCuH_p$' group around the B−Cu bond and the BH_3 group around the B_1-B_2 bond (Figure 3). The calculated activation energy barrier for this rearrangement is higher than for that previously described (about 14 and 11 kcal mol^{-1} at the MP2 and DFT levels, respectively). These two latter mechanisms are less favorable than the first one. Otherwise, they are inconsistent with the NMR spectra because they indicate the presence of two distinct boron environments. The study of the rearrangement between the **3a** and **3c** structures allows us to locate the **TS_4** transition state in total-potential-energy surface at both the MP2 and DFT levels of calculations. The calculated **3a → 3c** activation energy barrier is small (5.18 and 2.85 kcal mol^{-1} at MP2 and DFT levels, respectively), whereas the reverse isomerization appears to occur with negligible activation barrier (0.2 kcal mol^{-1}). This result shows that rearrangement of the **3c** structure to the most stable conformation is very fast. Finally, the activation energy for the isomerization between the less stable structures, **3b** and **3c,** was also found to be very small. The activation energy at MP2 and DFT levels are respectively 1.18 and 0.6 kcal mol^{-1} for the **3b → 3c** rearrangement, and 0.3 and 0.6 kcal mol^{-1} for the reverse rearrangement (**3c → 3b**). In Figure 5, we have summarized the energy profile for the $[ClCuB_3H_8]^-$ isomerization at DFT level.

Conclusion

The MP2 and DFT studies show that the $[ClCuB_3H_8]^-$ (**3a**) structure prefers the η^2 coordination mode for the $[B_3H_8]^-$ ligand toward the Cu metal. This structure is similar to that of B_4H_{10} borane, replacing the $[BH_2]^+$ group with the CuCl fragment. The $[ClCuB_3H_8]^-$ DFT vibrational frequencies are in good agreement with those observed experimentally and with those of $(PPh_3)_2CuB_3H_8$. The favorable internal rearrangement of this structure results from an intramolecular exchange between the bridged and terminal hydrogens. The involved activation energy is small. This is in good agreement with the NMR spectra and confirms the fluxional behavior of this complex. The rearrangement of the less stable structure, (**3c**), to the most stable structure, (**3a**), appears to occur with a negligible activation barrier. Finally, the calculated-activation-energy barriers of the rearrangement between the less stable structures were also found to be very small.

Acknowledgment. This work was partially supported by the Programme de CoopérationInteruniversitaire Maroco-Espanol (project 52P-00).

References and Notes

(1) Lippard, S. J.; Ucko, D. A. *Chem. Commun.* **1967**, 983.
(2) Lippard, S. J.; Ucko, D. A. *Inorg. Chem*. **1968**, *7*, 1051.
(3) Lippard, S. J.; Melmed, K. M. *Inorg. Chem.* **1969**, *8*, 2755.
(4) Muetterties, E. L.; Peet, W. G.; Wegner, P. A.; Alegranti, C. W. *Inorg. Chem.* **1970**, *9*, 2474.
(5) Borlin, J.; Gaines, D. F. *J. Am. Chem. Soc*. **1972**, *94*, 1367.
(6) Calabress, J. C.; Gaines, D. F.; Hildebrandt, S. J.; Morris, J. H. *J. Am. Chem. Soc*. **1976**, *98*, 5489.
(7) Klamberg, F.; Muetterties, E. L.; Guggenberger, L. J. *Inorg. Chem.* **1968**, *7*, 7272.
(8) Hildebrandt, S. J.; Gaines, D. F. *J. Am. Chem. Soc*. **1976**, *96*, 5574.
(9) Hildebrandt, S. J.; Gaines, D. F.; Calabress, J. C. *Inorg. Chem*. **1978**, *17*, 790.
(10) Hertz, R. K.; Goetze, R.; Shore, S. G. *Inorg. Chem*. **1979**, *18*, 2813.
(11) Alcock, N. M.; Burns, I. D.; Claire, K. S.; Hill, A. F. *Inorg. Chem.* **1992**, *31*, 2906.
(12) Burns, I. D.; Hill, A. F.; Williams, D. J. *Inorg. Chem.* **1996**, *35*, 2685.
(13) Bown, M.; Fontaine X. L. R.; Greenwood, N. N.; Mackinnon, P.; Kennedy, J. D.; Pett, M. J. *J. Chem. Soc., Dalton Trans*. **1987**, 2781.
(14) Pulham, C. R.; Downs, A. J.; Rankin, H.; Robertson, H. E. *J. Chem. Soc., Chem. Com*. **1990**, 1520.
(15) Beckett, M. A.; Jones, P. W. *Synth. React. Inorg. Met. -Org. Chem.* **1997**, *27*, 41.
(16) Burns, I. D.; Hill, A. F.; Thompsett, A. R. *J. Organometallics Chem.* **1992**, *C8*, 425.
(17) Serrar, C.; Es-sofi, A.; Boutalib, A.; Ouassas, A.; Jarid, A. *Inorg. Chem.* **2000**, *39*, 2224.
(18) Hill, T. G.; Godfroid, R. A.; White, J. P., III; Shore, S. J. *Inorg. Chem.* **1991**, *30*, 2952.
(19) Frisch, J.; Trucks, G. W.; Schlegel, H. B.; Gill, P. M. W.; Johnson, B. G.; Robb, M. A.; Cheeseman, J. R.; Keith, T.; Petersson, G. A.; Montgomery, J. A.; Raghavachari, K.; Al-Laham, A.; Zakrzewski, V. G.; Ortiz, J. V.; Foresman, J. B.; Peng, C. Y.; Ayala, P. Y.; Chen, W.; Wong, M. W.; Andres, J. L.; Replogle, E. S.; Gomperts, R.; Martin, R. L.; Fox, D. J.; Binkley, J. S.; Defrees, D. J.; Baker, J.; Stewart, J. P.; Head-Gordon, M.; Gonzalez, C.; Pople, J. A. *GAUSSIAN 94;* Gaussian, Inc.: Pittsburgh, PA, 1995.
(20) Becke, A. D. *Phys. Rev. A*. **1988**, *38*, 3098.
(21) Becke, A. D. *J. Chem. Phys*. **1993**, *98*, 5648.
(22) Lee, C.; Yang, W.; Parr, R. G. *Phys. Rev. B* **1988**, *37*, 785.
(23) Fukui, K. *J. Phys. Chem*. **1985**, *74*, 4161.
(24) Ishida, K.; Morokuma, K.; Komornicki, A. *J. Chem. Phys.* **1977**, *66*, 2153.
(25) Reed, A. E.; Curtiss, L. A.; Weinhold, F. *Chem. Rev.* **1988**, *88*, 899.
(26) Peters, C. R.; Nordman, C. E. *J. Am. Chem. Soc*. **1960**, *82*, 5758.
(27) Mitchell, G. F.; Welch, A. J. *J. Chem. Soc., Dalton. Trans*. **1987**, 1017.
(28) Binder, H.; Wolfer, K.; Fret, B.; Deiseroth, H. J.; Sommer, O. Z. *Anorg. Allg. Chem.* **1989**, *571*, 21.
(29) Serrar, C.; Es-sofi, A.; Boutalib, A.; Ouassas, A.; Jarid, A. *J. Mol. Struct. (THEOCHEM)* **1999**, *491*, 161.
(30) Bühl, M.; Schleyer, P. v. R. *J. Am. Chem. Soc*. **1992**, *114*, 477.
(31) Pepperberg, I. M.; Dixon, D. A.; Lipscomb, W. N., Halgren, T. A. *Inorg. Chem.* **1978**, *17*, 587.
(32) Nordman, C. E.; Lipscomb, W. N. *J. Chem. Phys.* **1953**, *21*, 1856.